Supporting Information for "Origins of Uncertainty in the Response of the Summer North Pacific Subtropical High to CO_2 Forcing"

Kezhou Lu[1], Jie He[1], and Isla R. Simpson[2]

[1]School of Earth and Atmospheric Sciences, Georgia Institute of Technology, Atlanta, GA, USA

[2]National Center for Atmospheric Research, Boulder, CO, USA

Contents of this file

1. Figures S1 to S15
2. Tables S1 and S2

Introduction: This file contains the following information: 1. a summary of all CMIP models used; 2. comparison of MMM response of ΔNPSH and ΔPr between Abrupt4 × CO_2 and AMIP 4 × CO_2+Future; 3. inter-model deviation of ΔNPSH from MMM for individual models; 4. inter-model spread of ΔNPSH in AMIP models; 5. descriptions of SWmodel and CAM5; 6. inter-model PCs of ΔNPSH and ΔSST; 7. intermediate results from tropical ΔSST inter-model spread experiment; 8. inter-model analysis of a subset of CMIP models; 9. ΔSST associated with IPCs of ΔNPSH; 10. inter-model spread of upper-level circulation response from CMIP/AMIP outputs; 11. role of extra-tropical land warming and transient eddies; 12 relationship between inter-model spread of ΔTS over land and inter-model spread of ΔNPSH; 13. inter-model spread of ΔPrecip over the North Pacific.

Table S1: Summary of CMIP5 and CMIP6 models

CMIP5			
No.	**Model Name**	**Resolution (atmosphere)**	**AMIP output available?**
1	ACCESS1-0	$1.875°EW \times 1.25°NS$, 38 levels	No
2	ACCESS1-3	$1.875°EW \times 1.25°NS$, 38 levels	No
3	bcc-csm1-1	T42, 26 levels	Yes
4	bcc-csm1-1-m	T106, 26 levels	No
5	CCSM4	$0.9°EW \times 1.25°NS$, 30 levels	Yes
6	CNRM-CM5-2	TL127, 31 levels	No
7	CNRM-CM5	TL127, 31 levels	Yes
8	CSIRO-Mk3-6-0	T63, 18 levels	No
9	GFDL-ESM2M	M45, 24 levels	Yes (GFDL-CM4)
10	GISS-E2-H	$2.5°EW \times 2°NS$, 40 levels	No
11	GISS-E2-R	$2.5°EW \times 2°NS$, 40 levels	No
12	HadGEM2-ES	N96, 38 levels	Yes (HadGEM2-A)
13	inmcm4	$2°EW \times 1.5°NS$, 21 levels	No
14	IPSL-CM5A-LR	$3.85°EW \times 1.875°NS$, 39 levels	Yes
15	IPSL-CM5A-MR	$2.5°EW \times 1.25°NS$, 39 levels	No
16	IPSL-CM5B-LR	$3.85°EW \times 1.875°NS$, 39 levels	Yes
17	MIROC5	T85, 40 levels	No
18	MIROC-ESM	T85, 40 levels	No
19	MPI-ESM-LR	T63, 47 levels	Yes
20	MPI-ESM-MR	T63, 95 levels	Yes
21	MPI-ESM-P	T63, 47 levels	No
22	MRI-CGCM3	TL159, 48 levels	Yes
23	NorESM1-M	f19, 26 levels	No
24	NorESM1-ME	TL159, 48 levels	No
CMIP6			
No.	**Model Name**	**Resolution (atmosphere)**	**AMIP output available?**
25	ACCESS-CM2	N96, 85 levels	No
26	ACCESS-ESM1-5	N96, 85 levels	No
27	AWI-CM-1-1-MR	T127, 95 levels	No
28	BCC-ESM1	T42, 26 levels	Yes (BCC-CSM2-MR)
29	CAMS-CSM1-0	T106, 31 levels	No
30	CanESM5	T63, 49 levels	Yes
31	CESM2	$1.25°EW \times 0.9°NS$, 32 levels	Yes
32	CESM2-FV2	$2.5°EW \times 1.9°NS$, 32 levels	No
33	CESM2-WACCM	$1.25°EW \times 0.9°NS$, 70 levels	No
34	EC-Earth3-AerChem	TL255, 91 levels	No
35	EC-Earth3-Veg	TL255, 91 levels	No
36	FGOALS-f3-L	c96, 32 levels	No
37	GISS-E2-1-G	$2.5°EW \times 2°NS$, 40 levels	No
38	GISS-E2-1-H	$2.5°EW \times 2°NS$, 40 levels	No
39	GISS-E2-2-G	$2.5°EW \times 2°NS$, 40 levels	No

40	IITM-ESM	T62, 64 levels	No
41	KACE-1-0-G	N96, 85 levels	No
42	MIROC6	T85, 81 levels	Yes
43	MRI-ESM2-0	TL195, 80 levels	Yes
44	NorCPM1	$2.5°EW \times 1.9°NS$, 26 levels	No
45	NorESM2-MM	$1°EW \times 1°NS$, 32 levels	No
46	TaiESM1	$1.25°EW \times 0.9°NS$, 30 levels	No

Figure S1 and S2. Multi-model ensemble mean (MMM) comparison between Abrupt$4 \times CO_2$ and AMIP$4 \times CO_2$+Future.

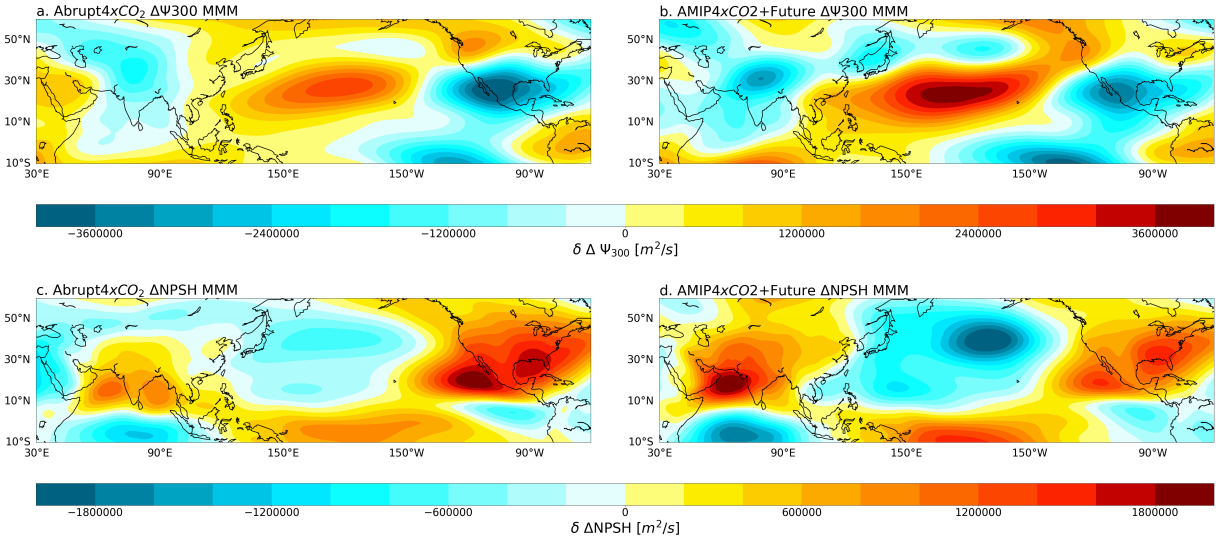

Figure S1. MMM response of 300-hPa eddy streamfunction (upper channel) and NPSH (lower channel) from 46 Abrupt4xCO_2 models (**a, c**) and 15 AMIP4xCO_2+Future scenarios (**b, d**). NPSH is represented by 850-hPa eddy streamfunction.

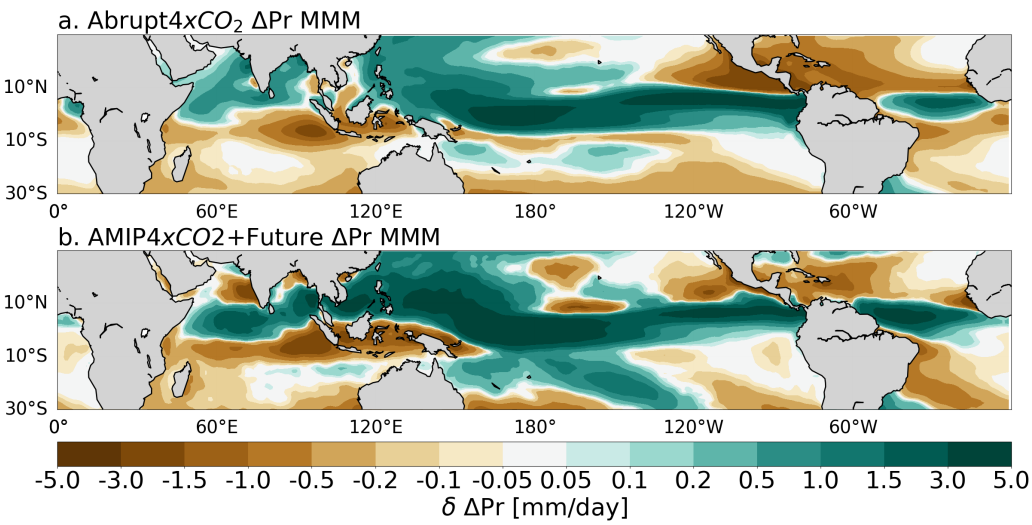

Figure S2. Similar to Figure S1 but for tropical precipitation.

Figure S3 and S4. Deviation from the multi-model mean of ΔNPSH equilibrium response for each individual model.

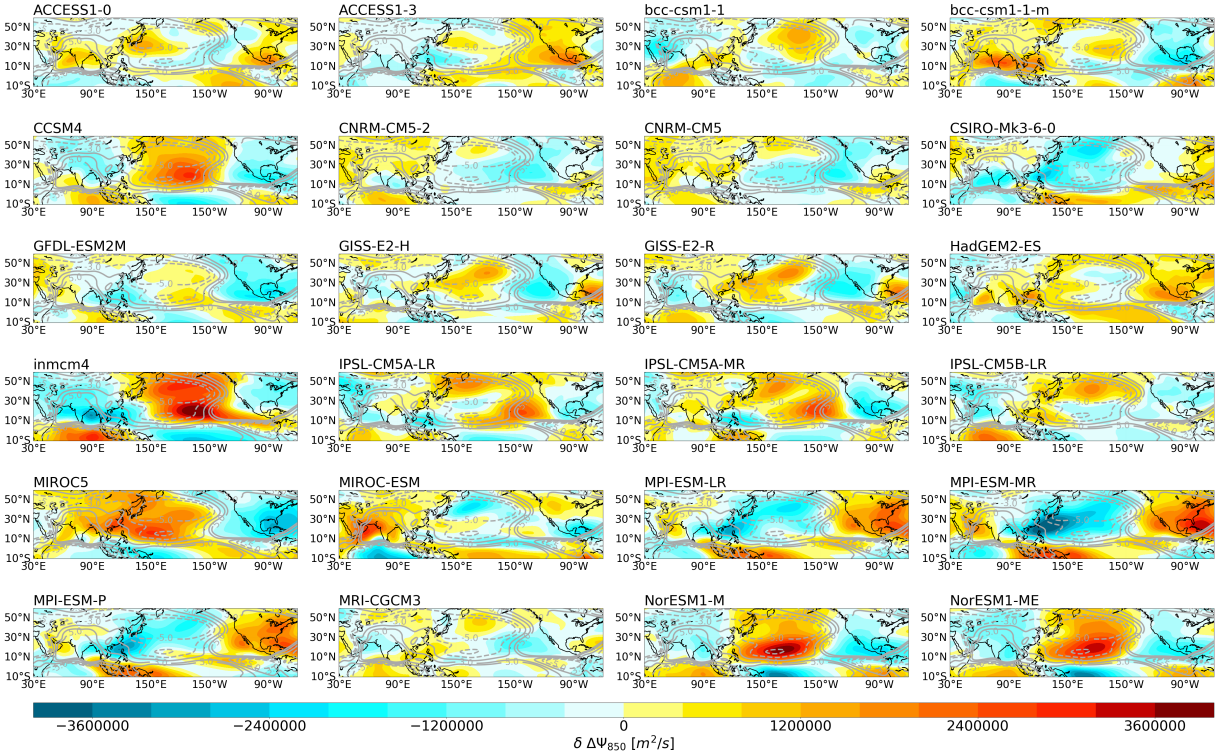

Figure S3. Deviation (shadings; m^2/s) from the multi-model mean (contours; $10^5 m^2/s$) of $\Delta\Psi_{850}$ equilibrium response for each individual model in CMIP5 and CMIP6 abrupt4×CO_2 simulation.

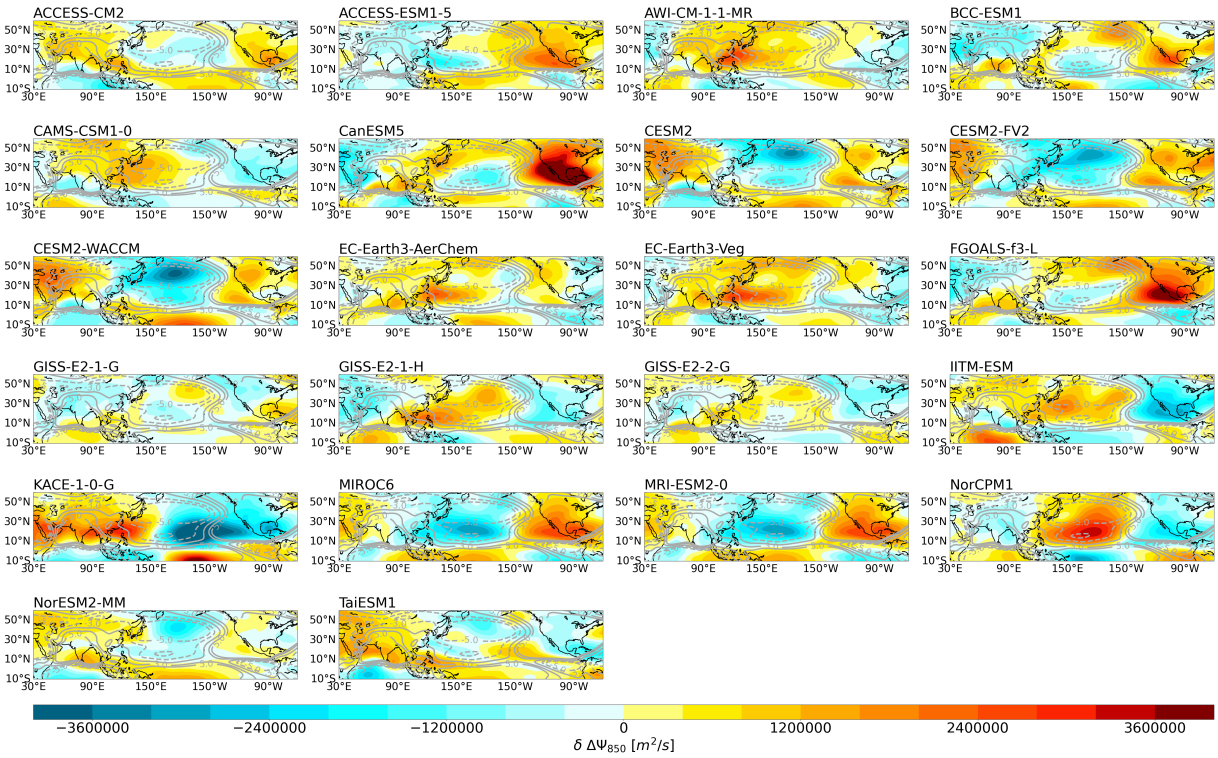

Figure S3. continued.

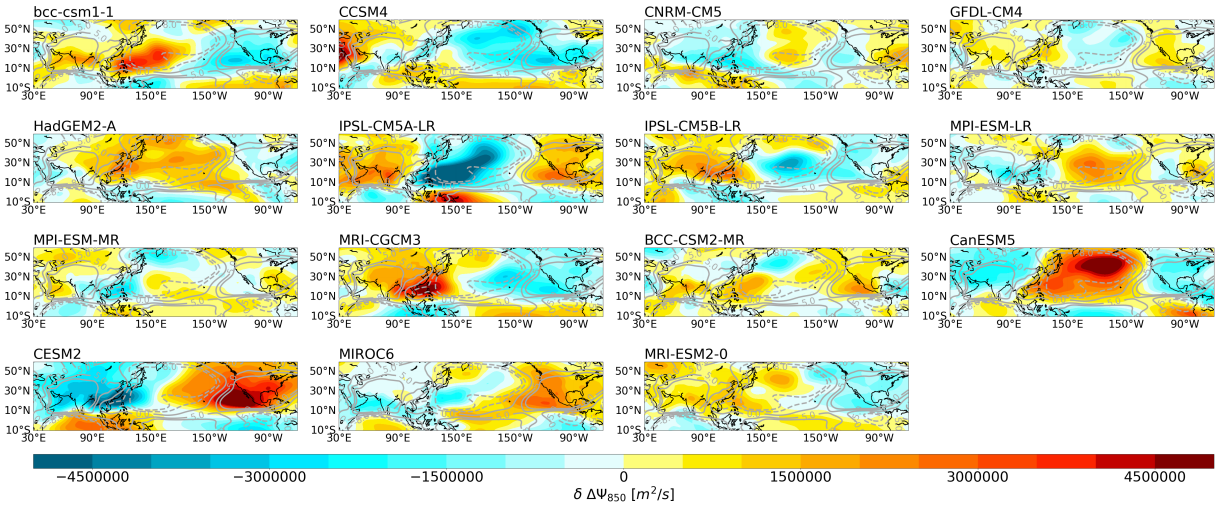

Figure S4. Same as Figure S3 but for AMIP4×CO_2+Future simulation.

Figure S5. Inter-model spread of ΔNPSH among AMIP models.

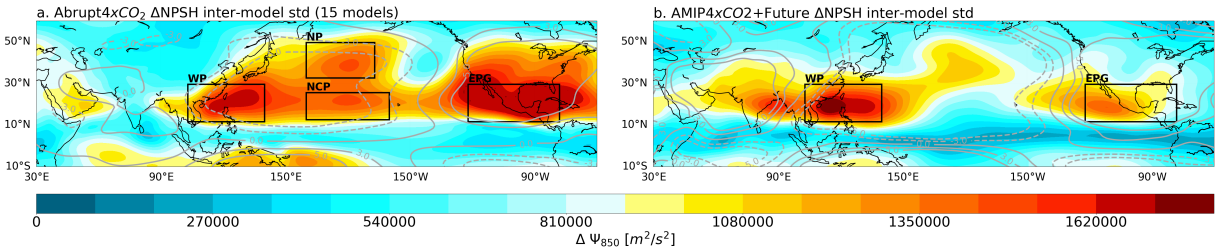

Figure S5. Inter-model standard deviation of ΔNPSH calculated from 15 Abrupt4 × CO_2 models with AMIP outputs (**a**) and 15 models under AMIP4 × CO_2+Future (**b**).These models are highlighted in red in Table S1.

Table S2: Model descriptions

	SWmodel	**CAM5**
Horizontal resolution	Rhomboidal wavenumber-30 truncation	FV 1-degree grid for both land and atmosphere
Vertical resolution	14 sigma levels	30 hybrid levels
Anomaly model	Yes	No
Damping coefficients	Rayleigh friction and Newtonian cooling is 15 days at all levels, and the biharmonic diffusion coefficient is 1 $\times 10^{17} m^4 s^{-1}$	Do not apply
Moist processes	Prescribed separately as an independent diabatic heating	Included
Transient eddies	Prescribed separately as an independent transient momentum forcing	Included
Topography	Prescribed separately if using zonal-mean basic state, otherwise embeded in the 3D basic state	Included
SST and sea ice	Do not apply	Prescribed
Interaction with land	Do not apply	Included

Figure S6. IPC1 of ΔNPSH and IPC1 of ΔSST in Abrupt$4 \times CO_2$ models.

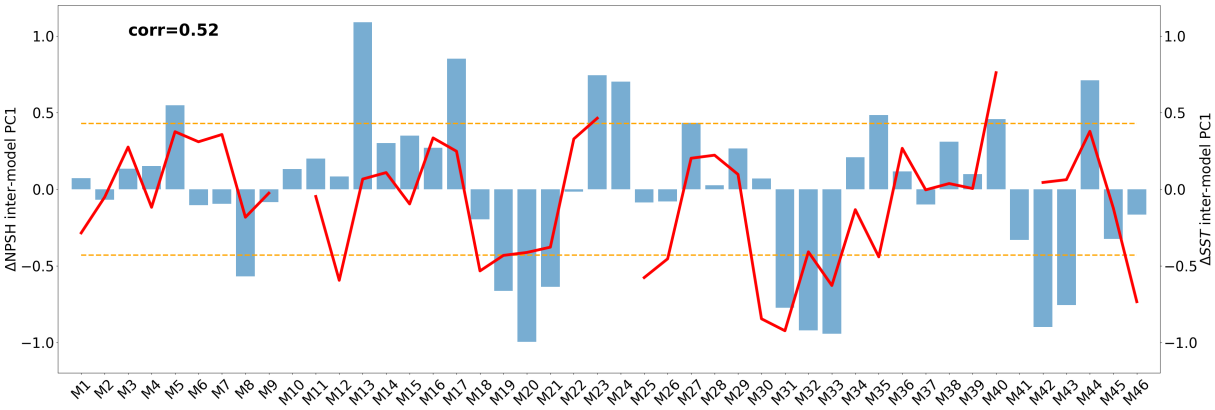

Figure S6. IPC1 of ΔNPSH (blue bars) and IPC1 of tropical ΔSST (red lines) from 46 fully coupled abrupt4×CO_2 models. The numbers (Mx) on the horizontal axis correspond to different models listed in Table S1. The correlation coefficient between IPC1 of ΔNPSH and IPC1 of ΔSST is 0.52. The orange line denotes the one standard deviation of the ΔNPSH PC1, and models that surpass this value are chosen to perform the composite analysis.

Figure S7: Intermediate results of tropical inter-model SST spread experiment from CAM5

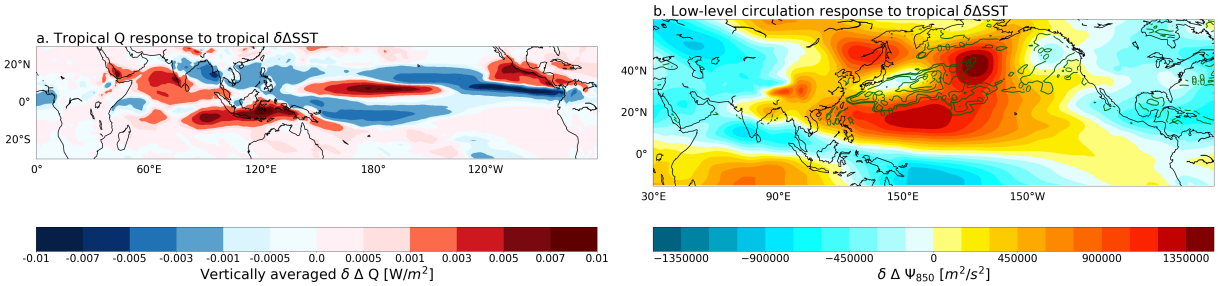

Figure S7. Response of total diabatic heating (Q) and low-level circulation to prescribed $\delta\Delta$SST in CAM5. **a** Vertically averaged response of Q (shadings). **b** Response of NPSH (shadings) and subtropical precipitation (contours; mm/day).

Figure S8: Inter-model spread of ΔNPSH captured by 15 CMIP models with AMIP outputs.

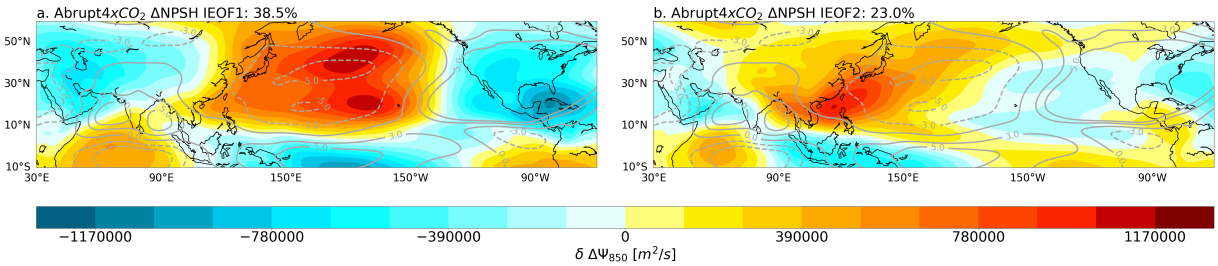

Figure S8. **a** and **b** Same as Figure 1c and 1d but produced by a subset of 15 CMIP models with AMIP outputs. These models are: bcc-csm1-1, CCSM4, CNRM-CM5, GFDL-ESM2M, HadGEM2-ES, IPSL-CM5A-LR, IPSL-CM5B-LR, MPI-ESM-LR, MPI-ESM-MR, MRI-CGCM3, BCC-ESM1, CanESM5, CESM2, MIROC6, and MRI-ESM2-0

Figure S9: Inter-model spread of ΔSST associated with IPC2 of ΔNPSH under Abrupt$4 \times CO_2$.

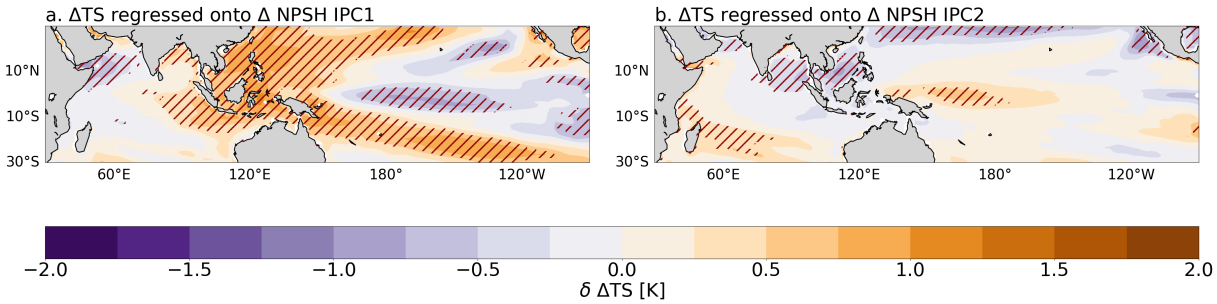

Figure S9. Regression of tropical ΔSST) onto the first (**a**) and second (**b**) inter-model principal components (IPCs) of ΔNPSH based on 46 Abrupt$4 \times CO_2$ models. Regions with statistically significant correlation are hatched.

Figure S10: Inter-model spread of $\Delta\Psi_{300}$ from both Abrupt$4\times CO_2$ and AMIP$4\times CO_2$+Future scenario.

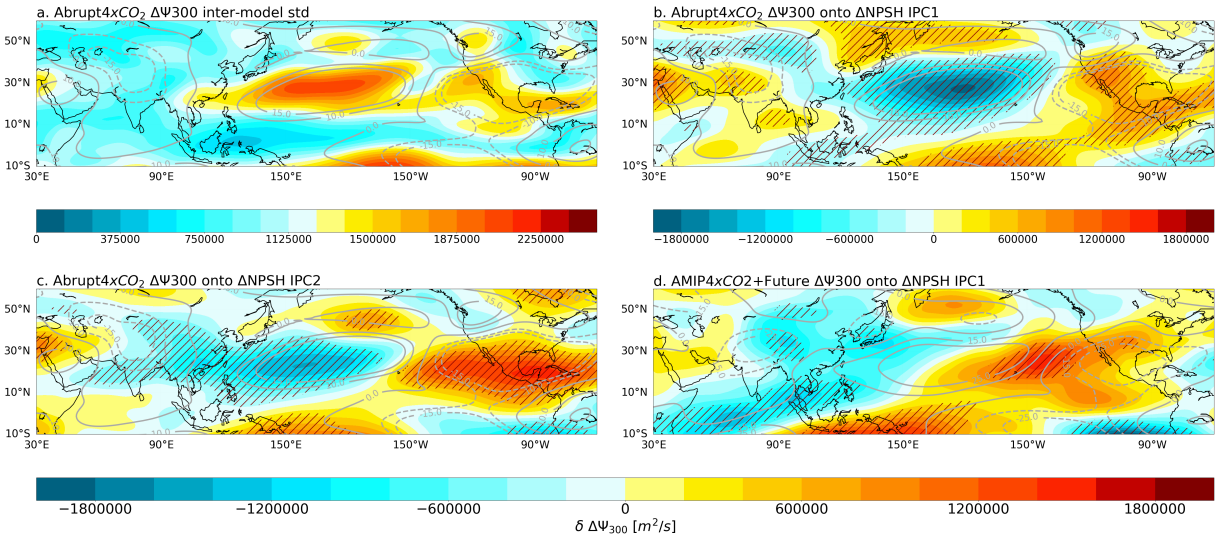

Figure S10. Similar to Figure 1 but for changes in 300-hPa eddy streamfunction regressed onto IPCs of ΔNPSH under Abrupt$4\times CO_2$ (**b,c**) or under AMIP$4\times CO_2$+Future (**d**).

Figure S11 and S12: Role of extratropical land warming and transient eddies in SWmodel

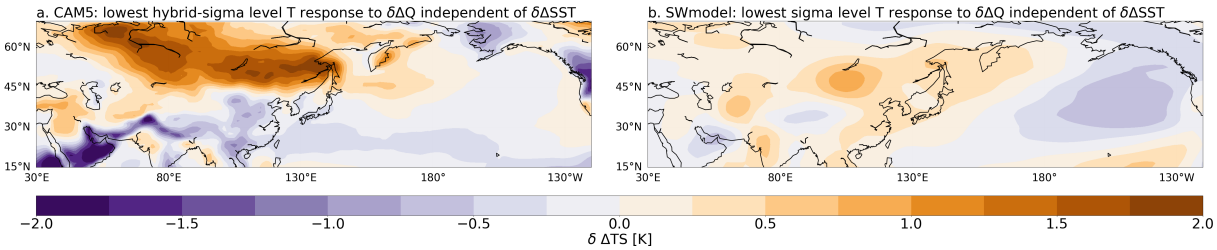

Figure S11. Response of air temperature at the lowest hybrid-sigma (or sigma) level to non-$\delta\Delta$SST induced tropical diabatic heating spread in CAM5 (a) and SWmodel (b).

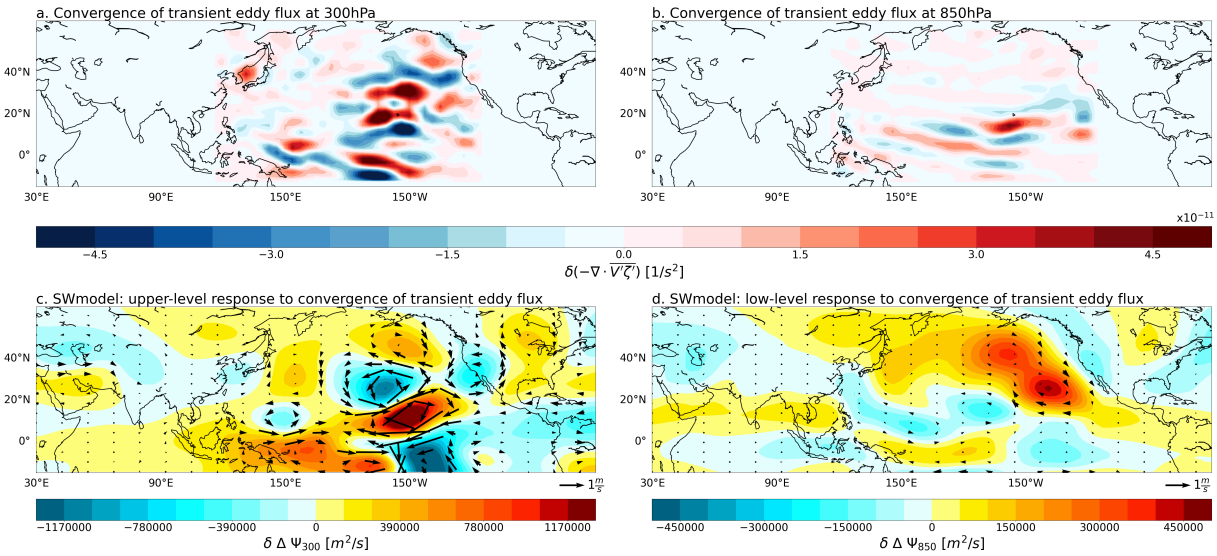

Figure S12. Role of convergence of transient eddy flux ($-\nabla \cdot \overline{\mathbf{v}'\xi'}$). The transient eddy flux can be calculated as: $-\nabla \cdot \overline{\mathbf{v}'\xi'} = -\frac{\partial^2 \overline{u'v'}}{\partial x^2} + \frac{\partial^2 \overline{u'^2}}{\partial x \partial y} - \frac{\partial^2 \overline{v'^2}}{\partial x \partial y} + \frac{\partial^2 \overline{u'v'}}{\partial y^2}$, where u', v' are daily zonal and meridional wind response to $\delta\Delta$SST induced $\delta\Delta$Q from CAM5. The transient vorticity forcing at 300 hPa and 850 hPa are shown in a and b. The response of 300-hPa eddy streamfunction and NPSH to this transient eddy momentum forcing simulated by SWmodel are shown in c and d. The effect of transient eddy flux could amplify the low-level anticyclone response around the NP and the barotropic structure North of $40°N$.

Figure S13 and S14: Inter-model spread of ΔTS over extra-tropical Eurasia and its relationship with ΔNPSH.

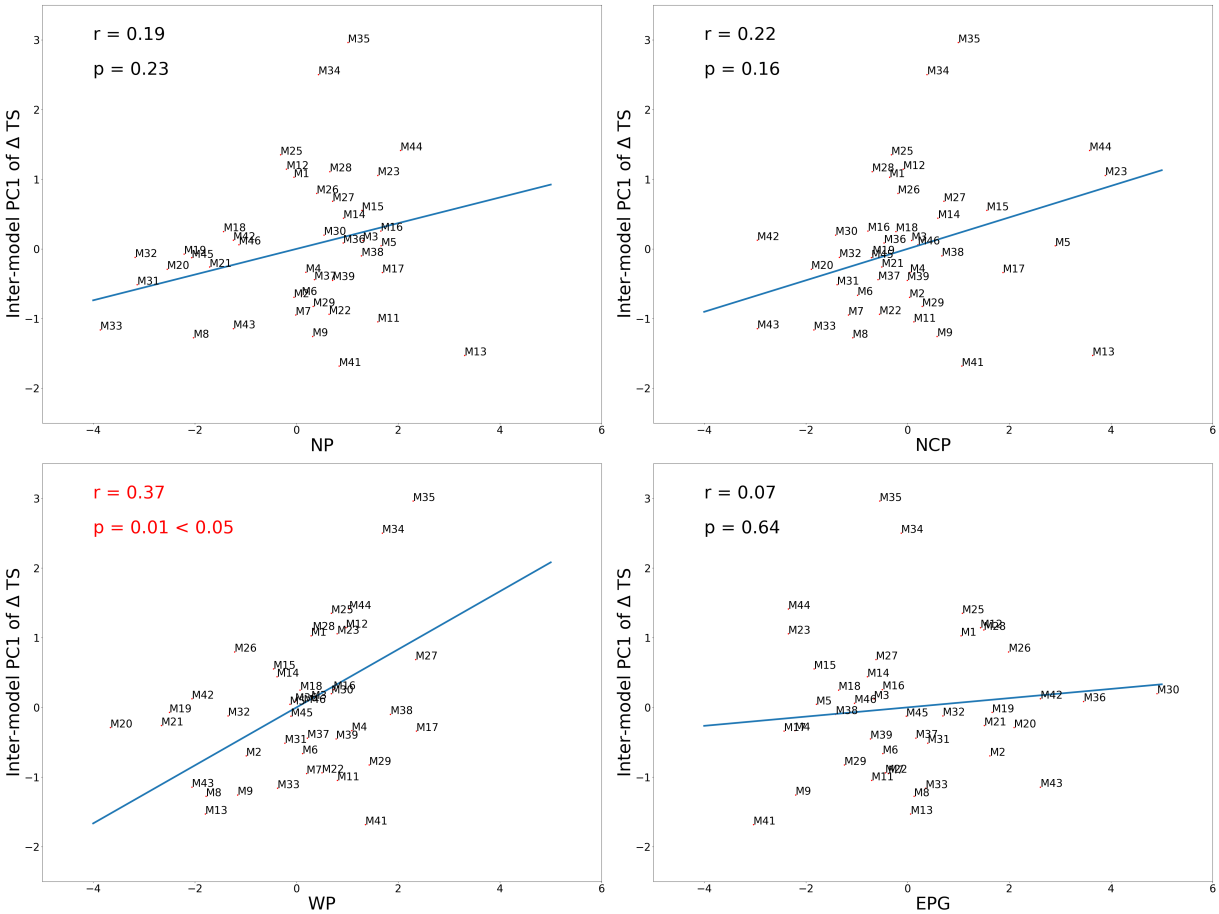

Figure S13. Correlation between the IPC1 of land ΔTS over extratropical Eurasia (20-60°N and 60-140°E) and ΔNPSH inter-model index averaged over NP (**a**), NCP (**b**), WP (**c**) and EPG (**d**). The ΔNPSH inter-model index is normalized by $1.25 \times 10^6 m^2/s$. The Pearson correlation coefficient r and the corresponding p-value are noted on each subplot. The inter-model correlation is considered significant when $p < 0.05$.

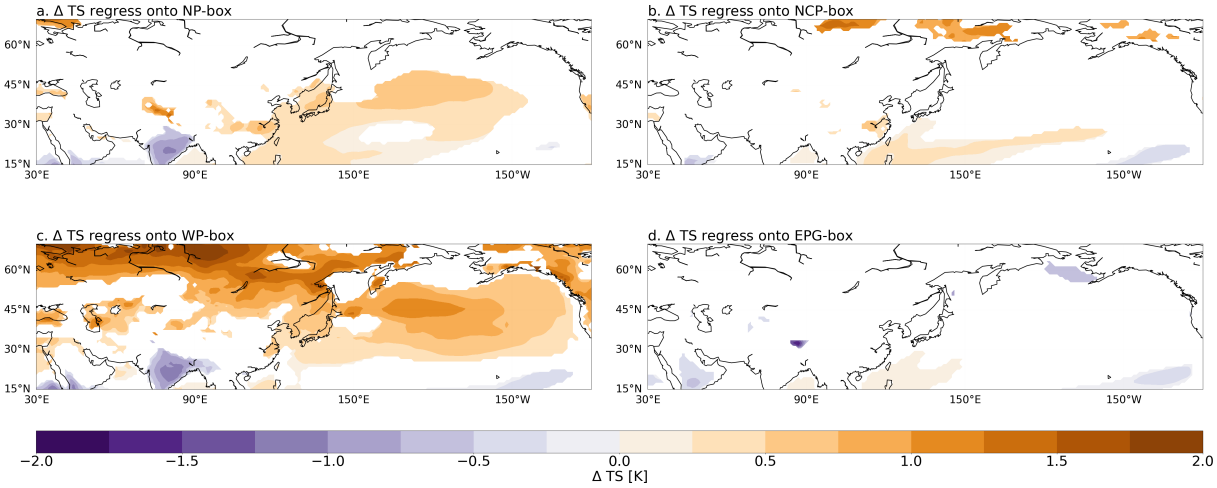

Figure S14. Regression map of ΔTS onto δΔNPSH index averaged over NP (**a**), NCP (**b**), IWP (**c**) and EPG (**d**). Only regions with significant correlations are plotted.

Figure S15: Inter-model spread of ΔPrecip over North Pacific.

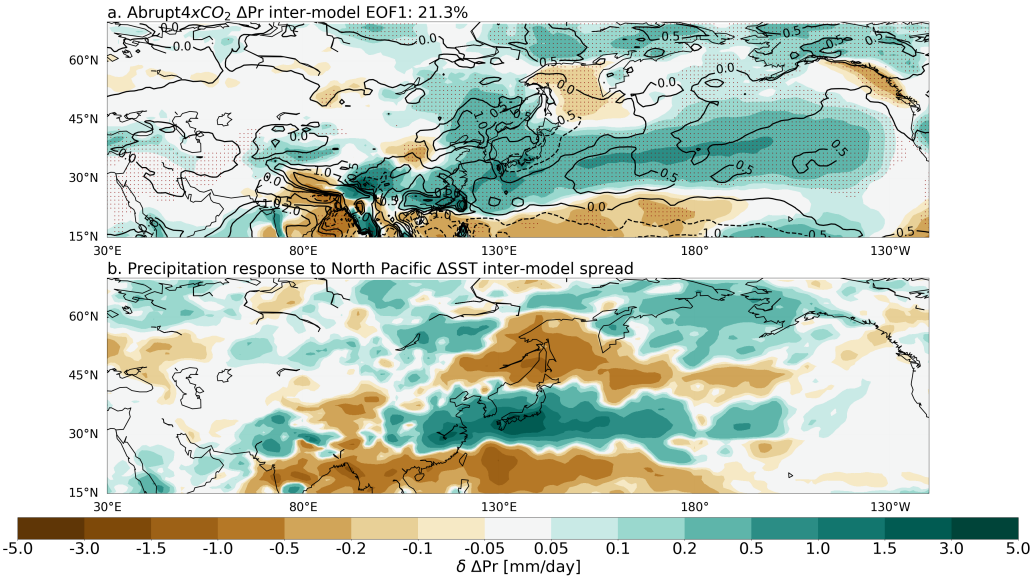

Figure S15. **a** Similar to Figure 2b but calculated over extra-tropical region. **b** The precipitation response to North Pacific inter-model ΔSST spread in CAM5.